**The Company of Biologists**

## RESEARCH ARTICLE

# Asymmetric distribution of hypoxia-inducible factor α regulates dorsoventral axis establishment in the early sea urchin embryo

Wei-Lun Chang[1,2,*], Yi-Cheng Chang[1,*], Kuan-Ting Lin[1], Han-Ru Li[1], Chih-Yu Pai[1], Jen-Hao Chen[1] and Yi-Hsien Su[1,2,‡]

## ABSTRACT

Hypoxia signaling is an ancient pathway by which animals can respond to low oxygen. Malfunction of this pathway disturbs hypoxic acclimation and can result in various diseases, including cancers. The role of hypoxia signaling in early embryogenesis remains unclear. Here, we show that in the blastula of the sea urchin *Strongylocentrotus purpuratus*, hypoxia-inducible factor α (HIFα), the downstream transcription factor of the hypoxia pathway, is localized and transcriptionally active on the future dorsal side. This asymmetric distribution is attributable to its oxygen-sensing ability. Manipulations of the HIFα level entrained the dorsoventral axis, as the side with the higher level of HIFα tends to develop into the dorsal side. Gene expression analyses revealed that HIFα restricts the expression of *nodal* to the ventral side and activates several genes encoding transcription factors on the dorsal side. We also observed that intrinsic hypoxic signals in the early embryos formed a gradient, which was disrupted under hypoxic conditions. Our results reveal an unprecedented role of the hypoxia pathway in animal development.

KEY WORDS: Hypoxia, HIFα, Dorsoventral patterning, Sea urchin embryo

## INTRODUCTION

Oxygen is essential for the survival of aerobic organisms. In animal cells, several signaling pathways can be activated for coping with low-oxygen environments (Semenza, 2007; Simon and Keith, 2008). The major hypoxia pathway involves the bHLH-PAS family transcription factor hypoxia-inducible factor α (HIFα) (Schofield and Ratcliffe, 2004) and is an ancient mechanism that is likely to be present in all animals (Loenarz et al., 2011). The stability and transcriptional activity of HIFα are regulated by oxygen-dependent hydroxylases (Kaelin and Ratcliffe, 2008). Under normal oxygen conditions (normoxia), HIFα is hydroxylated by prolyl hydroxylases (PHDs) at the key proline residues located in the conserved oxygen-dependent degradation domain (ODDD). This hydroxylation event results in the binding of HIFα to von Hippel-Lindau (VHL), a component of an E3 ubiquitin ligase complex, which leads to degradation of HIFα protein. The transcriptional activity of HIFα is modulated by factor inhibiting HIF (FIH), an asparaginyl hydroxylase that hydroxylates HIFα at the conserved asparagine residue in the C-terminal transactivation domain (CAD) to prevent it from binding to its co-factor p300. Under hypoxic conditions, the activities of these hydroxylases are inhibited, resulting in the formation of the HIFα and HIFβ (ARNT) heterodimer, which recognizes hypoxia-response elements (HREs) in downstream genes. In addition to hypoxia, other growth factor-activated signaling pathways and reactive oxygen species (ROS) also modulate the function of HIFα (Wenger et al., 2005).

The roles of the hypoxia pathway have been studied in several model organisms. In the nematode *Caenorhabditis elegans*, although HIFα (*hif-1*) mutants have no phenotype under laboratory conditions, unlike the wild type they are unable to survive and reproduce under low-oxygen conditions (Jiang et al., 2001). Similar results were observed in *Drosophila melanogaster*, in which the HIFα (*sima*) mutant is unable to adapt to hypoxia but is viable under normoxia (Centanin et al., 2005). Three HIFα paralogs have been identified in vertebrates (Rytkonen et al., 2011). In mouse, *Hif1a* knockout is embryonic lethal, with defects in neural tube and cardiovascular development (Iyer et al., 1998; Ryan et al., 1998). Knockout of *Hif2a* (*Epas1*) also results in embryonic or perinatal lethality with multiple organ pathology (Compernolle et al., 2002; Peng et al., 2000; Scortegagna et al., 2003; Tian et al., 1998). In addition to their roles in development, HIF1α and HIF2α are closely associated with cancer metastasis and other diseases (Rankin and Giaccia, 2016; Semenza, 2000). Much less is known about HIF3α; multiple variants have been found that differ in their regulation and functions (Duan, 2016). Despite the in-depth studies in physiology and disease, very little is known about the role of the hypoxia pathway in early embryogenesis.

One of the crucial events during early embryogenesis in animals is the establishment of the body axes. For bilaterians, proper dorsoventral (DV) axial patterning results in their bilaterally symmetric bodies. In echinoderm embryos, a redox gradient is involved in DV patterning (Coffman and Denegre, 2007). Studies during the 1940s demonstrated that redox inhibitors were effective in orienting the bilateral plane of sand dollar embryos (Pease, 1941, 1942a,b). The most inhibited region becomes dorsal, and the least inhibited region ventral. At approximately the same time, C. M. Child monitored the intracellular indophenol oxidase activity and observed regional differences in echinoderm blastula embryos (Child, 1941). Czihak further demonstrated that an activity gradient of the mitochondrial enzyme cytochrome oxidase is present as early as the 8-cell stage (Czihak, 1963). Using a fluorescent probe, it has been shown that the distribution of the mitochondria is asymmetric in unfertilized sea urchin eggs and the embryo; the side inheriting more mitochondria has a strong bias toward becoming the ventral side. Embryos cultured under hypoxia are defective in ectoderm specification along the DV axis (Agca et al., 2009; Coffman et al., 2004). Results from these studies

[1]Institute of Cellular and Organismic Biology, Academia Sinica, Taipei 11529, Taiwan. [2]Graduate Institute of Life Sciences, National Defense Medical Center, Taipei 11490, Taiwan.
*These authors contributed equally to this work

‡Author for correspondence (yhsu@gate.sinica.edu.tw)

K.-T.L., 0000-0002-3015-4858; Y.-H.S., 0000-0001-6798-9632

DEVELOPMENT

demonstrated that DV patterning in echinoderm embryos is intimately associated with the oxidative system.

There has been increasing interest in how the oxidative system is linked to gene regulatory networks (GRNs) that provide causal linkages between transcription factors and genomic regulatory sequences (Davidson, 2006). The expression of *nodal*, the upstream regulator of the ventral ectoderm GRN (Saudemont et al., 2010; Su et al., 2009), is downstream of the redox gradient (Coffman et al., 2004, 2014). p38 signaling, which responds to various environmental stimuli, including redox changes, is transiently inactivated on the dorsal side of sea urchin embryos and is required for *nodal* expression (Bradham and McClay, 2006). Several transcription factor binding sites, including those for redox-sensitive bZIP factors, have been found in the 5′ *cis*-regulatory module of the *nodal* gene (Nam et al., 2007; Range et al., 2007). Other maternal factors that seem to be unrelated to the redox gradients also regulate *nodal* expression. Analyses of the *cis*-regulatory elements further showed that SoxB1, a ubiquitously expressed maternal factor, and the maternal Wnt and Univin signals are also required for activation of *nodal* expression (Range et al., 2007). Recently, a TGFβ ligand named Panda has been shown to be a maternal factor that is preferentially localized on the dorsal side and that restricts *nodal* expression (Haillot et al., 2015). Therefore, several redox-sensitive and redox-insensitive regulatory factors are required for the correct spatial and temporal expression of the sea urchin *nodal* gene in order to properly orient the DV axis. However, to date, no redox-sensitive transcription factors related to sea urchin DV axial patterning have been identified.

We have previously shown that mRNA of sea urchin *hifα* is ubiquitously distributed in the early blastula. Knockdown of HIFα slightly reduced dorsal expansion of the pluteus larva and decreased the expression of *tbx2/3* and *dlx*, which contain HREs and are normally expressed on the dorsal side of the blastula (Ben-Tabou de-Leon et al., 2013; Chen et al., 2011). Nevertheless, it is unclear how the ubiquitously localized *hifα* transcript is specifically involved in the dorsal ectoderm GRN. In this study, we reveal that the *S. purpuratus* HIFα protein is preferentially stabilized in the dorsal half of the blastula. We also report the regulation and function of HIFα and show that hypoxia treatments disrupt the asymmetric distribution of HIFα and the intrinsic hypoxia gradient.

## RESULTS
### Sea urchin HIFα is preferentially degraded on one side of the blastula
HIFα is known to be regulated at the protein level, and we therefore aimed to examine HIFα protein distribution during embryogenesis. We generated an mRNA encoding N-terminal Myc-tagged HIFα (Myc-HIFα) and injected it into the zygote. Immunostaining using a Myc antibody revealed that Myc-HIFα was preferentially located within nuclei (nuclearized) on one side of the blastula (Fig. 1A, Movie 1). This phenomenon is tightly associated with the amount of mRNA injected (Fig. 1B). When a low amount of mRNA (50-100 ng/µl) was injected, the asymmetric signal could be detected in 25% of the embryos, whereas when a moderate amount (100-150 ng/µl) was injected, more than half (53%) of the embryos displayed asymmetric distribution. Because the injected mRNA was expected to be distributed evenly in the embryo, the asymmetric distribution of HIFα suggests that the protein is synthesized or degraded preferentially in one half of the embryo. Further increasing the mRNA amount (150-175 ng/µl or above) resulted in strong, nuclearized signals in all blastomeres in 55% of embryos, whereas asymmetry was still observed in 45% of the embryos. The ability to

synthesize HIFα in all cells supports the hypothesis that the asymmetric distribution is regulated through differential protein degradation rather than translation. The fact that the asymmetry is highly sensitive to the amount of transcript present in the embryo implies that the activity of the protein degradation machinery is surpassed by an overdose of the mRNA.

To confirm that HIFα was preferentially degraded, embryos were co-injected with mRNAs encoding Histone-GFP and mCherry-HIFα fusion protein for live imaging (Fig. 1C). The GFP signal was observed as early as the 8-cell stage in every nucleus. Three hours later, at the 56-cell stage [7 h post fertilization (hpf)], the mCherry signal started to appear in some of the injected embryos. Similar to the GFP control, mCherry-HIFα was initially translated in every blastomere. At 9 hpf, when the GFP signal was still strong in every nucleus, the mCherry signal started to fade away in half of the early blastula and the asymmetry was maintained at 12 hpf. In embryos injected with mRNA encoding mCherry only, the signal was observed in every cell at all of the stages we examined and no differential degradation was detected (Fig. S1). The observation that HIFα was translated in every cell and then attenuated in half of the blastula strongly supports its degradation in one half of the embryo. A similar result could be seen in a time-lapse movie when observing a single embryo throughout early embryogenesis (Fig. 1D, Movie 2).

To quantify the fold difference in HIFα levels between the strong and weak sides, we normalized the mCherry signal to the GFP fluorescence intensity detected on each side. The initial mCherry-HIFα signal was ubiquitous and the maximum fold difference was 1.65 (Fig. 1E). We also observed that the asymmetry was transient and only lasted for a few hours. Quantification of more embryos injected with Myc-HIFα and Histone-GFP mRNA at the blastula stage (12 hpf) (Fig. 1F) revealed that the average fold difference between the sides with strong and weak HIFα levels was 1.69 ($n$=64), although the differences varied considerably (Fig. 1G), possibly owing to high sensitivity to the amount of mRNA injected. These results support the conclusion that the asymmetric distribution of HIFα is attributable to its preferential degradation.

### HIFα is preferentially nuclearized and transcriptionally active on the dorsal side
To investigate which side contained strong HIFα signals, we performed Myc staining in combination with *in situ* hybridization for *nodal*. This showed that the side with strong HIFα signal was mostly opposite to that of the *nodal* expression domain on the ventral side (Fig. 2A). To orient the embryo correctly, we further used a Vasa antibody, which labels primordial germ cells located at the vegetal pole (Voronina et al., 2008). In most of the embryos triple-labeled for Myc, *nodal* and Vasa, the strong HIFα signal was confirmed to be on the dorsal side (Fig. 2B).

To monitor the endogenous transcriptional activity of HIF, we injected a reporter construct containing three HREs upstream of firefly luciferase (HRE-Luc). Staining the embryos with a luciferase antibody revealed that luciferase was, in most cases, synthesized strongly in the region lacking *nodal* expression (Fig. 2C), suggesting that endogenous HIF is transcriptionally active on the dorsal side.

### Both hypoxia and DMOG disrupt HIFα asymmetry
The sea urchin genome encodes a complete suite of hypoxia pathway components, including one HIFα and one HIFβ, one FIH, two PHDs (PHDA and PHDB) and one VHL (Rytkonen et al., 2011). To investigate whether the components of this pathway are present during embryogenesis, we examined the expression of the genes. We
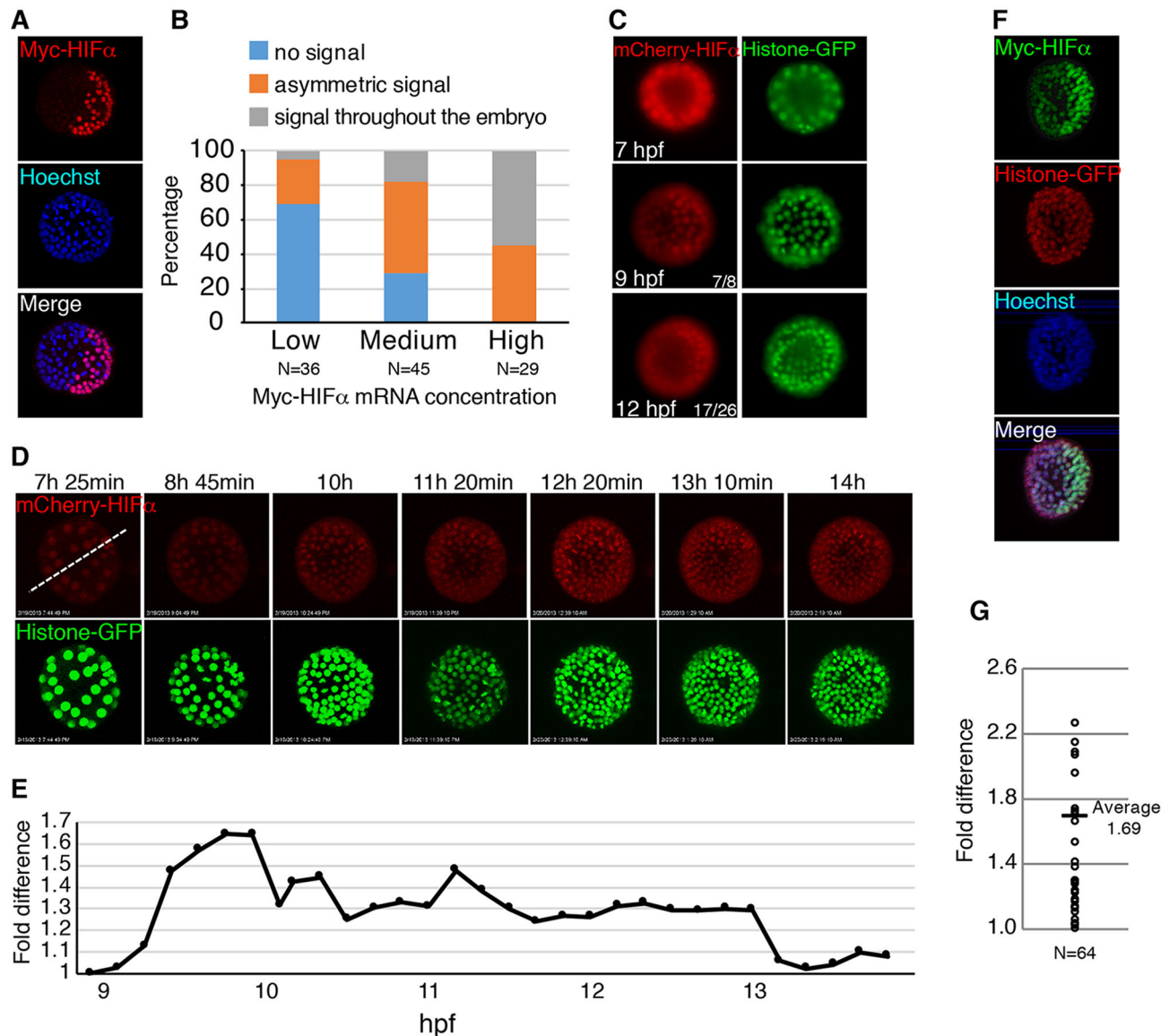
**Fig. 1. HIFα is preferentially degraded in one half of the sea urchin embryo.** (A) The blastula (12 hpf) injected with Myc-HIFα mRNA was stained with anti-Myc antibody and Hoechst 33342 for nuclei. (B) Myc staining patterns in embryos injected with different amounts of Myc-HIFα mRNA were quantified as no detectable signal, asymmetric signal in half of the embryo, or signal throughout the embryo. (C) Live imaging of embryos injected with mCherry-HIFα and Histone-GFP mRNA at the 56-cell (7 hpf) and early blastula (9 and 12 hpf) stages. (D) Representative images from a time-lapse recording during early embryogenesis. The dashed line demarcates the strong and weak HIFα sides observed at the blastula stage. (E) Quantification of fold differences between strong and weak HIFα signals during the course of the time-lapse recording. (F) Embryos (12 hpf) co-injected with Myc-HIFα and Histone-GFP mRNA were stained with Hoechst and antibodies against Myc and GFP at the blastula stage. (G) The fold differences between strong and weak were quantified using GFP intensity as a reference.

have shown previously that the *hifα* transcript is deposited maternally and distributed ubiquitously in the egg and early blastula (Ben-Tabou de-Leon et al., 2013). By further examining more refined stages, we confirmed that *hifα* mRNA is distributed evenly during cleavage stages (Fig. S2A). Quantitative PCR (QPCR) revealed that except for the *phda* transcript, which could not be detected before 24 hpf, transcripts of *hifβ*, *fih* and *phdb* were all present within the first day of development, although *hifβ* and *fih* mRNAs were only at very low levels (Fig. S2B). *In situ* hybridization analyses showed that *hifβ*, *phdb* and *vhl* transcripts were ubiquitously distributed in the egg and early blastula (Fig. S2C). These results confirmed that, except for *phda*, the complete suite of hypoxia pathway components is indeed present during early sea urchin embryogenesis and thus may participate in regulating HIFα.

Sea urchin HIFα contains all of the domains, with their conserved proline and asparagine residues, typical of vertebrate HIFα proteins (Fig. 3A), implying that it is regulated in a similar way. To investigate whether oxygen-dependent mechanisms control HIFα distribution, we cultured the Myc-HIFα-injected embryos in a hypoxic chamber until early blastula stage and performed Myc staining. The hypoxia treatment significantly disrupted HIFα asymmetry, with the signal becoming evenly distributed in every nucleus (Fig. 3B). This result suggests that, similar to the vertebrate HIFα proteins, sea urchin HIFα is stabilized under hypoxia. To further examine the role of the oxygen-dependent hydroxylases, the Myc-HIFα-injected embryos were treated with dimethyloxaloylglycine (DMOG), a competitive inhibitor of 2-oxoglutarate, one of the co-factors for PHDs and FIH hydroxylases (Foxler et al., 2012; Gomes et al., 2013). Similar to the
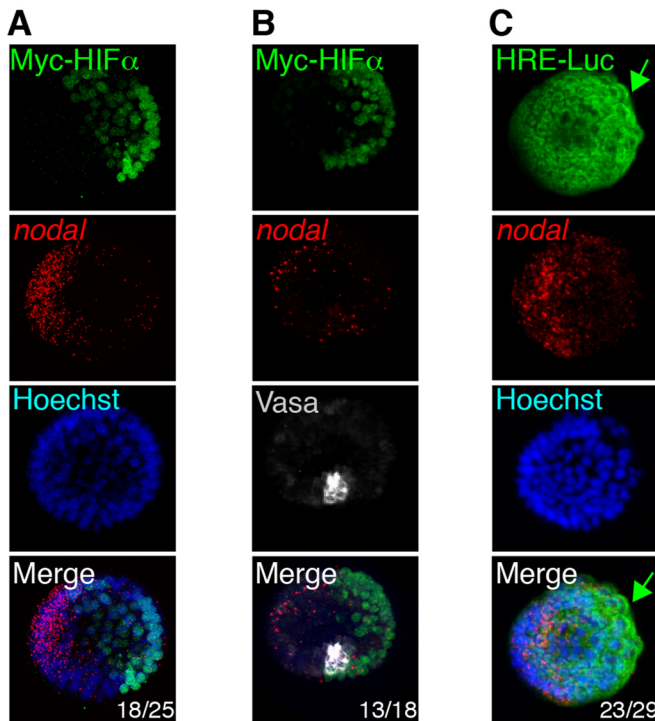
**Fig. 2. HIFα is nuclearized and transcriptionally active on the presumptive dorsal side of the blastula.** (A) Double staining for Myc and *nodal* transcript in a blastula injected with Myc-HIFα mRNA. (B) Triple staining for Myc, *nodal* transcript and Vasa protein in a blastula injected with Myc-HIFα mRNA. (C) Immunostaining using anti-luciferase antibody in a blastula injected with HRE-Luc reporter. The side with strong luciferase signal is indicated by the green arrow. The number showing the illustrated phenotype among the total examined is indicated.

hypoxia treatment, DMOG significantly blocked HIFα asymmetry in a dose-dependent manner (Fig. 3C). These results suggest that hydroxylase activities are involved in the differential distribution of HIFα.

### The asymmetric stabilization of HIFα is proline and asparagine dependent

To test whether proline and asparagine hydroxylations are involved in regulating the asymmetric stabilization of HIFα, we mutated the conserved residues to alanine. When the embryos were injected with mRNA encoding a single proline mutation (P417A or P530A), HIFα asymmetry was significantly disrupted (Fig. 4A,B). Double proline mutations (P417/530A) further decreased the difference in HIFα levels. Moreover, injections of the P417/530A HIFα resulted in stronger and more sustainable signals than injections of wild-type HIFα (Fig. 4C). The wild-type HIFα signal usually faded by 18 hpf, whereas the P417/530A HIFα signal was still prominent. These results strongly suggest that the differential distribution of HIFα is regulated by protein degradation via hydroxylation of the conserved proline residues by oxygen-sensitive PHDs. Interestingly, in embryos injected with the asparagine-mutated construct (N903A), although the difference was also significantly reduced, the overall Myc signal was weaker (Fig. 4A,B), suggesting that the conserved asparagine residue also contributes to the stability of the protein.

The fact that the conserved proline residues are important for the asymmetric stabilization of HIFα suggests that PHD activity, despite the ubiquitous distribution of *phdb* transcript, is also asymmetric along the DV axis. To monitor PHD activities, we generated a construct encoding a fusion protein containing the

ODDD of HIFα and GFP. The ODDD contains the conserved proline residues, and the distribution of ODDD-GFP has been used as a proxy for PHD inactive regions (Safran et al., 2006). In embryos co-injected with ODDD-GFP and mCherry-HIFα we observed that, similar to the HIFα signal, the ODDD-GFP was detected in half of the blastula, and the two signals were detected in the same cells in all of the embryos examined (Fig. 4D). These results suggest that the prospective dorsal side contains lower PHD activity leading to the stabilization of HIFα. The future ventral side, by contrast, has higher PHD activity, resulting in the hydroxylation and thus degradation of HIFα.

### The DV axis can be entrained when the HIFα level is perturbed

A previous study showed that the redox gradient of sea urchin embryos can be entrained when embryos are cultured in clusters (Coffman and Davidson, 2001). In embryos clustered in rosettes, the outside is more oxidative and contains more mitochondria, and that side tends to develop into the ventral side. To test whether HIFα asymmetry can also be entrained, we injected clustered embryos with mCherry-HIFα and Histone-GFP. In just over 50% of the embryos scored, HIFα was localized inside the clustered embryos, whereas GFP signals were evenly distributed (Fig. 5A,B). This result is consistent with the asymmetric distribution of HIFα on the prospective dorsal side. We further used MitoTracker, a cell-permeable probe that accumulates in active mitochondria, to label the injected embryos. As expected, in most cases MitoTracker labeled the outside of the rosettes, whereas HIFα was distributed toward the inside (Fig. 5C). These results support the idea that, similar to the redox gradient and mitochondrial distribution, the distribution of HIFα can be entrained in embryos clustered in rosettes.

A previous lineage-tracing experiment demonstrated that the DV axis of the sea urchin embryo is specified by the first cleavage (Cameron et al., 1989). We designed experiments to perturb the level of HIFα randomly on one side after the first cleavage. As shown previously (Ben-Tabou de-Leon et al., 2013), the HIFα morpholino (MO) reduced the extension of the dorsal apex in a dose-dependent manner (Fig. S3). The specificity of the MO was examined by co-injection with mRNA encoding wild-type or P417/530A HIFα (Fig. S4). The shortening of the body lengths caused by the MO could be rescued by either mRNA, demonstrating its specificity. We then injected the HIFα MO, together with Dextran-fluorescein (fluo) as a tracer, into one of the cells of 2-cell stage embryos. The injected embryos were observed at late gastrula stage, when the DV axis is easily distinguishable. In the fluo-injected control embryos, the side that inherited the tracer became either the ventral or the dorsal side at a nearly 1:1 ratio (Fig. 5D). Very few embryos showed the tracer on the right or left side. When HIFα MO was co-injected with the tracer, the side that inherited the MO showed a higher likelihood of developing into the ventral side (ventral:dorsal 1.82:1), which deviated significantly from that of the control (Fig. 5E). By contrast, when the MO was replaced with HIFα mRNA, the injected blastomere tended to become the dorsal side (dorsal:ventral 1.59:1). These results support the idea that HIFα plays a positive role on the dorsal side and that manipulation of its level entrains the DV axis.

### HIFα restricts *nodal* expression and activates dorsal genes

We have previously shown that *tbx2/3* and *dlx*, genes that are normally expressed in the dorsal ectoderm (dorsal genes), contain HREs and are downstream of HIFα (Ben-Tabou de-Leon et al., 2013). Here, we further examined the expression of genes that
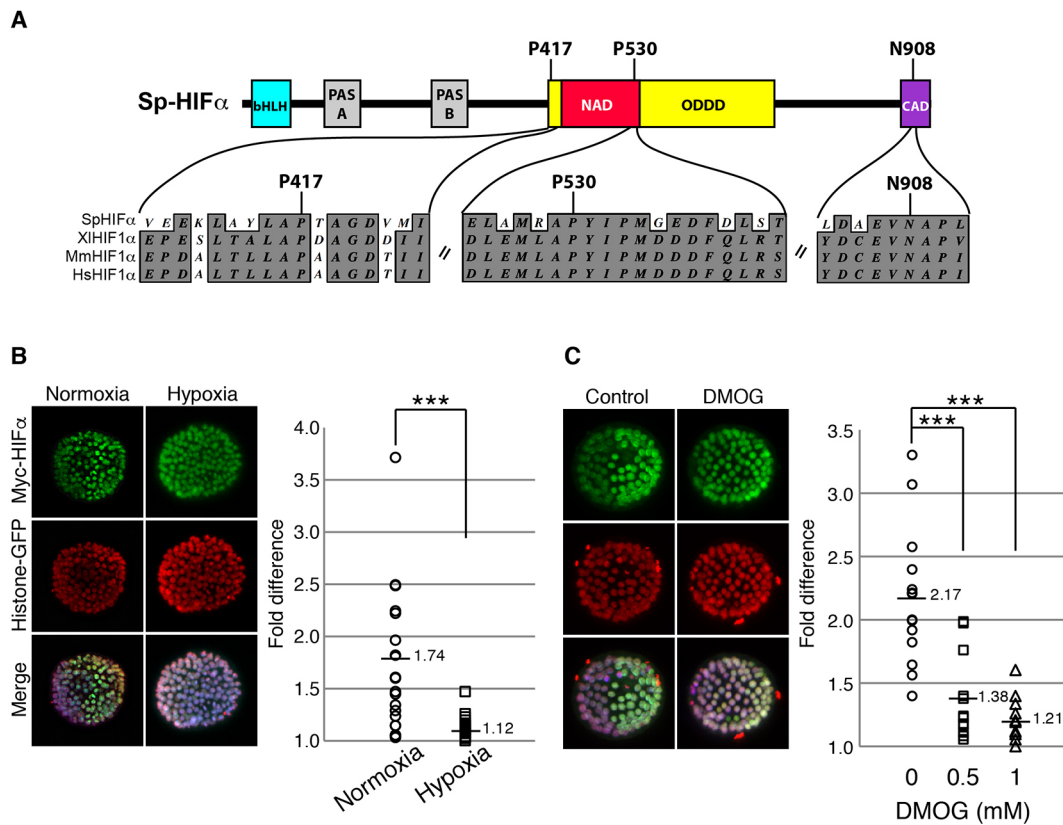
**Fig. 3. HIFα asymmetry is regulated by an oxygen-dependent mechanism.** (A) The domain structure of the sea urchin HIFα (Sp-HIFα) protein. The bHLH domain binds to DNA, the two PAS domains (PAS A and PAS B) are involved in heterodimerization, the two conserved proline residues are within the oxygen-dependent degradation domain (ODDD) containing the N-terminal transactivation domain (NAD), and the conserved asparagine residue is in the C-terminal transactivation domain (CAD). The sequences around the conserved hydroxylation sites of the sea urchin (Sp), *Xenopus laevis* (Xl, DQ529235), mouse (Mm, BC026139), and human (Hs, NM_001530) HIFα proteins are aligned. The conserved proline and asparagine residues are indicated, and the identical/similar residues are indicated by bold type and shading. (B) Embryos co-injected with Myc-HIFα and Histone-GFP mRNA were cultured under normoxia or hypoxia and stained with Myc and GFP antibodies at the blastula stage. Quantification of fold differences between strong and weak HIFα signals is shown to the right (*t*-test, ***$P<0.001$). (C) Embryos co-injected with Myc-HIFα and Histone-GFP mRNA were treated with DMOG, and quantification of fold differences is shown to the right (*t*-test, ***$P<0.001$).

constitute the DV ectodermal GRN upon perturbation of HIFα. By QPCR analyses, similar to published findings (Nam et al., 2007), we observed that *nodal* expression was initiated at 6-8 hpf, and its transcript level reached a peak at 10 hpf and then decreased slightly (Fig. 6). In HIFα knockdown embryos, the *nodal* transcript level kept increasing from 10 to 12 hpf, and the effect was still observed although attenuated in the hatched blastula (18 hpf). At 24 hpf (mesenchyme blastula), HIFα MO was no longer able to increase the *nodal* transcript level. The effective time window of the MO coincides with that of the presence of maternal HIFα. *In situ* hybridization analysis confirmed that the *nodal* expression domain expanded at 12 and 18 hpf, suggesting that HIFα helps in shaping the *nodal* expression domain in the early blastula. The expansion of the *nodal* expression domain caused by the MO could be rescued by mRNA encoding wild-type or P417/530A HIFα (Fig. S4). Downregulation of *tbx2/3* and *dlx* in embryos injected with HIFα MO was also observed (Fig. 6), confirming our previous results. In addition, the expression of *hmx*, another dorsal gene, was downregulated in HIFα morphants (Fig. 6). The expression of other genes in the GRN, such as the dorsal genes *msx* and *irxA* and the ventral genes *chordin*, *gsc* and *foxG*, was not consistently affected by HIFα MO (Fig. S5). These results suggest that the roles of HIFα on the dorsal side are in restricting *nodal* expression and in activating several genes encoding transcription factors within the GRN.

**The sea urchin embryo contains intrinsic hypoxic signals that form a gradient**

The results presented above show that, during sea urchin embryogenesis, PHD activity is higher on the ventral side and lower on the dorsal side and that this leads to the asymmetric distribution of HIFα on the dorsal side, which in turn regulates gene expression. To investigate whether hypoxia is intrinsic in the embryo, we incubated the embryos with pimonidazole, a hypoxia marker that binds to thiol-containing proteins in hypoxic environments (Varia et al., 1998). The pimonidazole-protein adducts were then detected by immunofluorescence. A gradient of fluorescent signals was observed in the pimonidazole-treated embryos cultured under normoxia (Fig. 7A). In embryos cultured under hypoxia, the gradient was disrupted and the signals became evenly distributed. We used Vasa localization to orient the embryos and observed that in more than 90% (46 out of 49) of the embryos examined, the gradient formed along an axis perpendicular to the animal-vegetal axis, possibly along the DV axis (Fig. 7B). Using 3D surface plot analyses, we clearly observed an intrinsic hypoxia gradient, whereas CellMask, a fluorescent dye for membrane staining, labeled every cell uniformly. These results suggest that differential PHD activity along the DV axis can be attributed to the presence of an intrinsic hypoxia gradient in the sea urchin blastula.
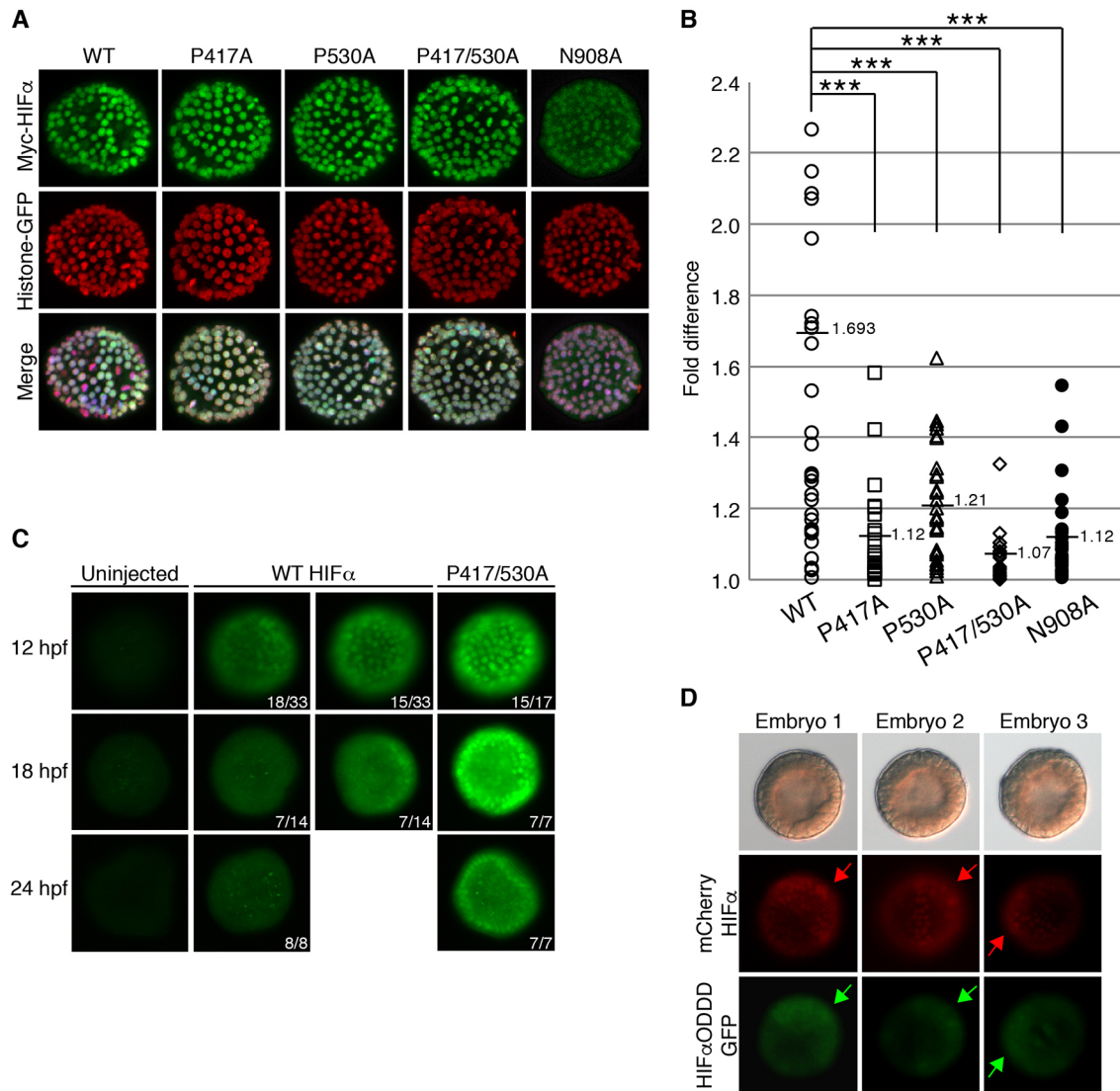
DEVELOPMENT

**Fig. 4. HIFα asymmetry is regulated by asymmetric PHD activity.** (A) Embryos co-injected with mRNAs encoding Histone-GFP and Myc-tagged wild-type (WT) or mutated HIFα were stained with Myc and GFP antibodies at the blastula stage. (B) Quantification of fold differences between strong and weak HIFα signals (t-test, ***P<0.001). (C) Uninjected embryos and embryos injected with mRNAs encoding Myc-tagged WT or P417/530A HIFα were stained with Myc antibody and observed at 12, 18 and 24 hpf. (D) Embryos co-injected with mCherry-HIFα and ODDD-GFP mRNA were observed under brightfield, TRITC and FITC filters. Three different embryos are shown and the areas showing the strongest fluorescent signals are indicated by arrows.

## DISCUSSION

### Hypoxia, redox, mitochondria and the regulation of HIFα

In this study, we have shown that transcripts encoding components of the hypoxia pathway are present during early embryogenesis in the sea urchin *S. purpuratus*. We also present evidence showing that HIFα is preferentially nuclearized and transcriptionally active on the future dorsal side, due to its degradation on the ventral side. HIFα asymmetry is regulated by oxygen-sensitive hydroxylases that are more active on the ventral side. HIFα distribution can be entrained in embryos cultured in clusters, and the DV axis of embryos can likewise be entrained when the HIFα level is manipulated. We have also observed that an intrinsic oxygen gradient is present in the blastula that may result in the preferential activation of the hypoxia pathway (Fig. 8). However, owing to technical difficulties, although we show that the oxygen gradient is perpendicular to the animal-vegetal axis, the oxygen gradient has not been confirmed to be along the DV axis. Further studies are required to clarify the

direction of the gradient and its causative link to the activation of the hypoxia pathway.

In cultured mammalian cells, HIF1α and HIF2α have been shown to be more stable in a reducing environment (Chen and Shi, 2008; Guo et al., 2008). In sea urchin embryos, the dorsal side is a more reducing environment (Coffman et al., 2004; Czihak, 1963). The redox gradient is proposed to be related to the asymmetric distribution of the mitochondria in the embryo. Mitochondria are not only the energy factory in cells but also generate ROS that can function in signal transduction. Under hypoxia, cells increase overall mitochondrial ROS levels but, paradoxically, the level of $O_2^{\cdot-}$, which is the dominant free radical species under normoxia, decreases when the oxygen concentration is reduced (Poyton et al., 2009). It has been suggested that the increased level of ROS under hypoxia is due to other free radical species, such as peroxynitrite ($ONOO^-$), the concentration of which increases under hypoxia. It has been proposed that hypoxia elevates ROS in the sea urchin embryo (Agca et al., 2009), although experimental measurements revealed
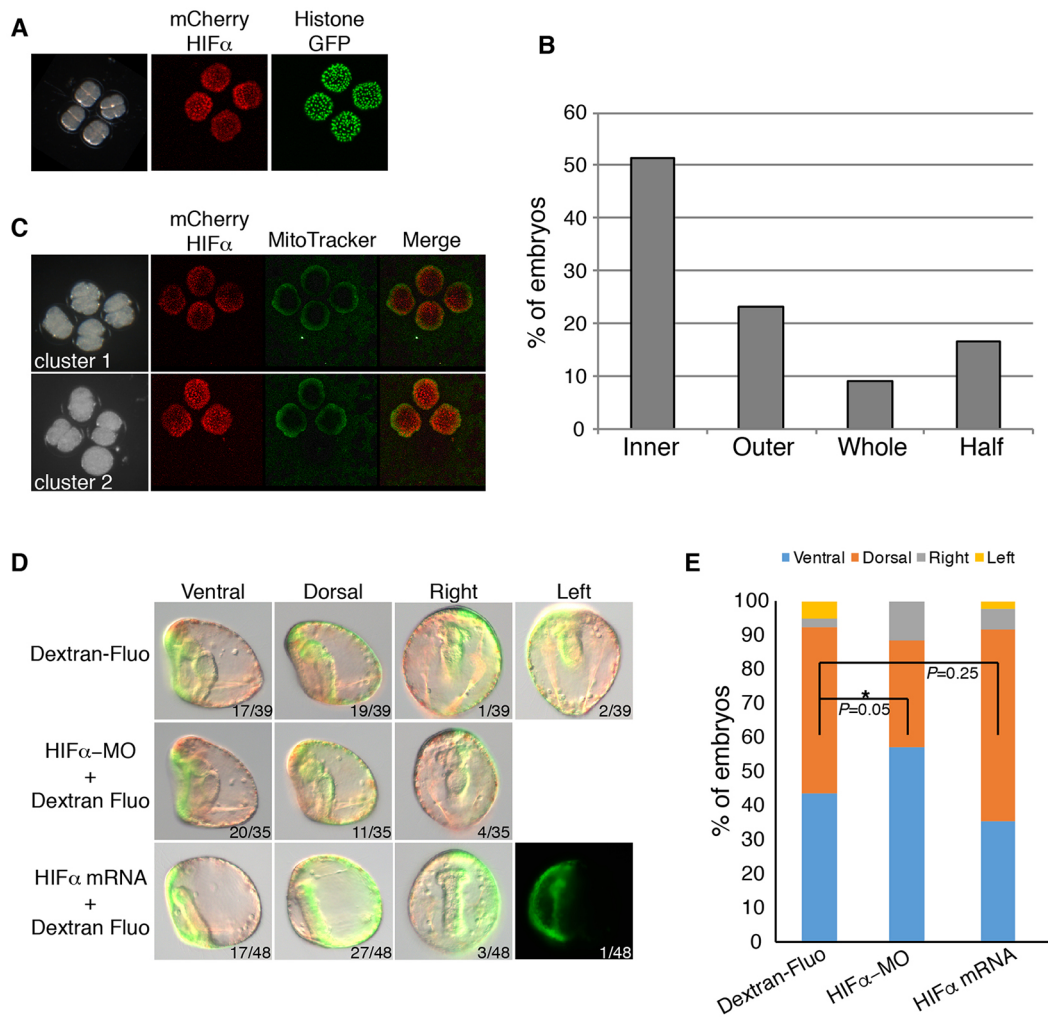
**Fig. 5. HIFα asymmetry and the DV axis can be entrained.** (A) Four embryos clustered in a rosette were injected with mCherry-HIFα and Histone-GFP mRNA. The left panel shows embryos at the 4-cell stage, and the mCherry and GFP signals were observed at the blastula stage. (B) The percentage of embryos in rosettes containing mCherry-HIFα signals in the inner portion of the embryo, the outer portion, whole, or half embryos (where could not be classified as inner or outer). (C) Clusters of embryos were injected with mCherry-HIFα mRNA and stained with MitoTracker at the blastula stage. (D) Dextran-fluorescein was injected without or with HIFα MO (100 µM) or mRNA (100 ng/µl) into one cell of the 2-cell embryo and observed at gastrula stage. (E) The percentage of embryos containing fluorescent signals was scored at gastrula stage. Chi-square statistics, using the ventral:dorsal ratio of the fluo-injected control embryos as the expected frequency (P, probability). The asterisk indicates that the ratio deviated significantly from that of the control.

that the $H_2O_2$ level decreases under hypoxia (Coluccio et al., 2011). Given that $H_2O_2$ can be converted from $O_2^{\bullet-}$ (Poyton et al., 2009), the observation in the sea urchin embryo is consistent with the notion that $O_2^{\bullet-}$ levels drops in low oxygen conditions. Regardless of the composition of free radical species, hypoxia-induced mitochondrial ROS modulate HIFα in different ways, including stabilization of HIFα in respiratory-incompetent cells (Bell et al., 2007; Poyton et al., 2009). In sea urchin embryos, fewer mitochondria and the reducing environment on the prospective dorsal side might be linked to the stabilization of HIFα. However, it is unclear whether the hypoxic signal that we observed relates to the redox gradient and mitochondrial distribution, and sources of the asymmetric HIFα activity remain unknown.

The unequal distribution of mitochondria or their activities in early development is a common feature in many animal species (Coffman and Denegre, 2007). A cytoplasmic structure called the Balbiani body or sponge body that contains various organelles including mitochondria was first discovered in the oocytes of spiders and myriapods and later in other arthropods (Kloc et al.,

2014). The Balbiani body has also been found in the oocytes of *Xenopus* and several vertebrate species (De Smedt et al., 2000). In *Xenopus* oocytes, the vegetally localized Balbiani body serves as a vehicle for transporting germplasm and several mRNAs that are involved in axial patterning (Kloc et al., 2001). In ascidians, a mitochondria-rich region of the egg forms a cytoplasmic domain called myoplasm that contains maternal determinants for muscle specification (Sardet et al., 2007). In most cases, it remains unclear how the unequal distribution of mitochondria contributes to animal development. Thus, our findings regarding sea urchin HIFα provide a possible link between mitochondrial asymmetry and axial patterning. Given that the unequal distribution of mitochondria is a common phenomenon, it is worth investigating whether an intrinsic oxygen gradient and HIFα asymmetry are also prevalent in other animals.

### Multiple pathways pattern the DV axis in sea urchins

With the establishment of the sea urchin ectodermal GRNs and recent studies on regulatory factors (Bradham and McClay, 2006; Chang
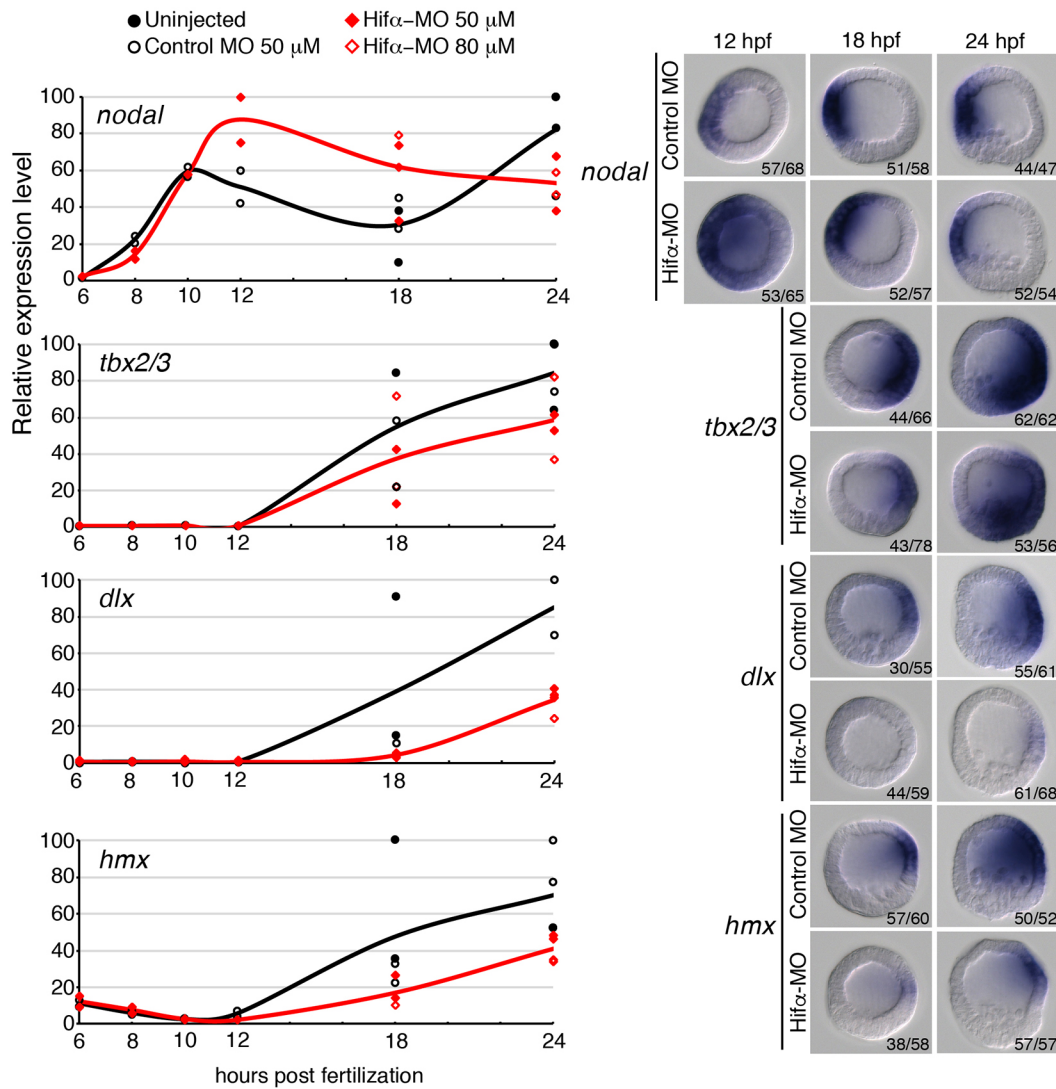
DEVELOPMENT

Fig. 6. Effects of HIFα MO on the expression of genes in the GRN. QPCR (left) and *in situ* hybridization (right) analyses were performed on embryos injected with control or HIFα MO. The y-axis of the QPCR data indicates the relative expression level, and the highest expression level in an individual experiment was designated as 100. Results from several independent experiments are presented and the lines represent average levels. Embryos are presented in lateral view with ventral to the left. The phenotype ratios shown bottom right are combined from three independent batches.

et al., 2016; Haillot et al., 2015; Lapraz et al., 2015; Saudemont et al., 2010; Su et al., 2009), it has become clear that multiple factors participate in patterning the DV axis. Our study shows that HIFα is an additional factor contributing to the DV patterning. Although the HIFα knockdown embryos contained shorter dorsal apexes, their DV axis is still distinguishable. Our gene expression analyses show that

knockdown of HIFα has a timely effect in restricting *nodal* expression and has only a minor effect on *tbx2/3*, which is activated mainly by BMP signals (Ben-Tabou de-Leon et al., 2013). Similarly, when the HIFα level was perturbed in one of the cells at the 2-cell stage, the ratio of the DV bias never surpassed 2:1 (∼67%). This observation is comparable to those from classical
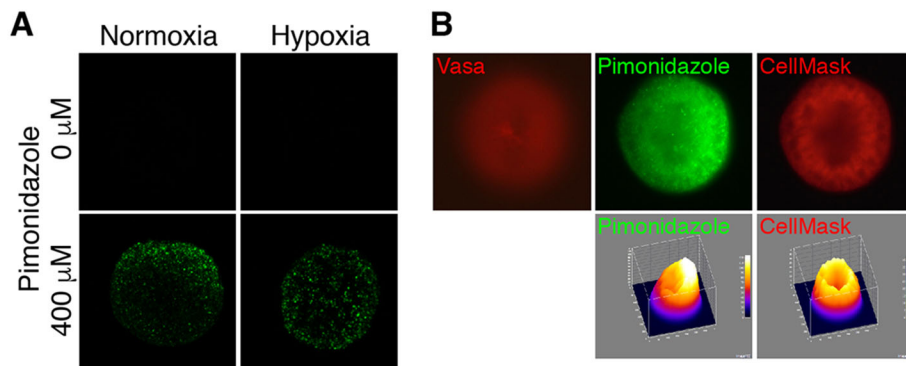


Fig. 7. An intrinsic hypoxia gradient in the blastula. (A) Blastula stage embryos incubated without or with pimonidazole cultured under normoxia or hypoxia were stained with an antibody targeting pimonidazole-protein adducts. (B) A sea urchin blastula stained with anti-Vasa, anti-pimonidazole-protein adduct antibody, or CellMask Deep Red. Beneath are 3D surface plots derived from the images above.
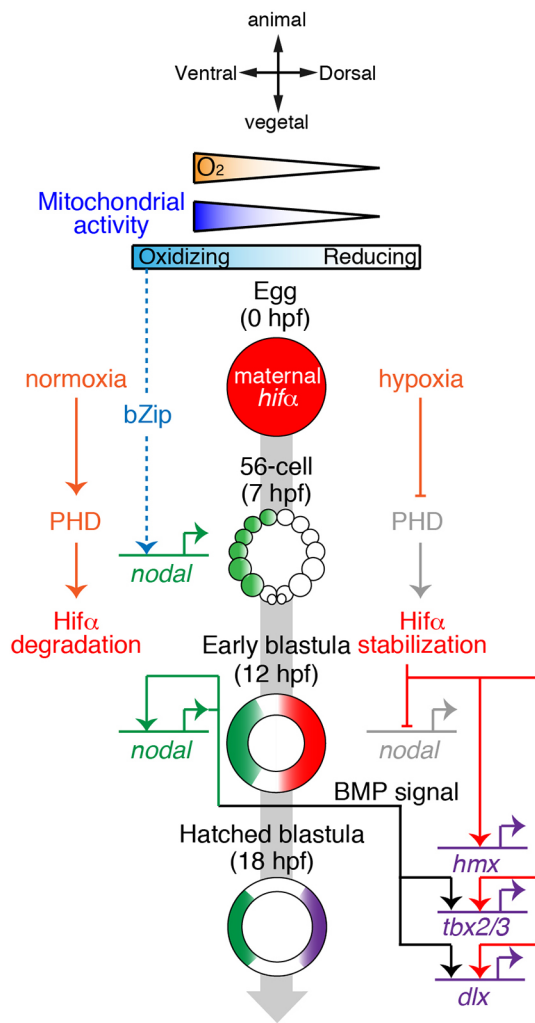
**Fig. 8. Model of DV axis formation in the *S. purpuratus* embryo.** The oxygen gradient, differential mitochondrial distribution, and the resulting redox gradient might differentially activate the enzymatic activity of PHDs and *nodal* gene expression, via a bZip factor, on the ventral side. Activation of PHDs leads to degradation of HIFα protein, which is translated from the ubiquitously distributed maternal *hifa* transcript. The presumably low oxygen environment on the dorsal side inhibits PHD activity and thus stabilizes HIFα protein. HIFα represses *nodal* expression and activates the expression of *hmx*, *tbx2/3* and *dlx*; the latter two are also activated by BMP signals, the ligand of which is a downstream gene of Nodal signaling.

studies using redox inhibitors (Pease, 1941, 1942a,b) and from more recent mitochondrial transfer experiments (Coffman et al., 2004). All these results suggest that the distribution of mitochondria, redox activity, and the asymmetric stabilization of HIFα provide positional bias, but not determinant, for DV patterning. It is currently unknown whether the positional information provided by HIFα interacts with other signals determining the DV axis. Because the DNA binding activity of human HIF1 is enhanced by TGFβ (Shih and Claffey, 2001), it would be intriguing to test whether sea urchin HIFα is modulated by Panda, a TGFβ ligand discovered in the sea urchin *Paracentrotus lividus* (Haillot et al., 2015).

A previous study showed that p38 signaling is transiently inactivated on the future dorsal side of the sea urchin *Lytechinus variegatus* embryo (Bradham and McClay, 2006). We have attempted to decipher the relationship between p38 inactivation and HIFα asymmetry. As reported in *L. variegatus*, we found that the p38 inhibitor SB203580 blocks *nodal* expression in *S.*

*purpuratus* (data not shown). However, SB203580 treatment had no effect on HIFα distribution, suggesting that p38 is not upstream of HIFα. We also tried to examine phospho-p38, which indicates active p38 signaling. Unfortunately, we observed uniform phospho-p38 signal in every nucleus and were unable to detect any transient disappearance. This might be due to the specificity of the phospho-p38 antibody or to species differences. Interspecies variation in the use of regulatory factors might be prominent during early development. A cross-species comparison of gene expression profiles between *S. purpuratus* and *P. lividus* has revealed a high level of conservation in the temporal order of gene activation but also cases of divergence (Gildor and Ben-Tabou de-Leon, 2015). For example, *gsc* is expressed initially at the blastula stage in *S. purpuratus*, whereas in *P. lividus* the *gsc* transcript is maternally deposited in the egg. Therefore, interspecies variation needs to be considered and our current data cannot exclude the possibility that HIFα participates in the inactivation of p38 signaling, although parallel pathways are also possible.

In our study, we observed minor changes in DV axial patterning in HIFα knockdown embryos, and no recognizable phenotypical changes were detected in embryos overexpressing wild-type or P417/530A HIFα. This differs from published observations in which embryos cultured in hypoxic environments develop a radialized phenotype (Coffman et al., 2004, 2014). Therefore, hypoxia treatment has a broader effect, possibly via other HIFα-independent pathways. Indeed, it has been shown that hypoxia causes circumferential expression of *nodal* in *S. purpuratus* embryos (Coffman et al., 2014), and this effect apparently surpasses the repression of the *nodal* gene by HIFα. In other model organisms, it has also been reported that several HIF-independent pathways provide important hypoxic adaptations. In mammals, the oxygen-sensitive mTOR energy-sensing pathway and the unfolded protein response (UPR) pathway are required during development (Simon and Keith, 2008). In *C. elegans*, the oxygen-binding soluble guanylate cyclase and the sensory cGMP-gated ion channel mediate oxygen sensation and control a social feeding behavior (Gray et al., 2004). Therefore, disruption of the sea urchin DV axis by hypoxia is likely to be attributable to multiple pathways.

## Development is both genetically determined and physiologically/environmentally controlled

Animal development has long been thought of as robustly controlled by a genetic program built into the genome. However, recent studies on developmental plasticity have provided many examples showing that environmental factors play important roles (Beldade et al., 2011). In aerobic organisms, oxygen is an essential environmental factor. Under physiological conditions, oxygen levels of different human organs/tissues vary and are usually lower than that of atmospheric air (Carreau et al., 2011). So-called 'physiological hypoxia' is also observed in the uterine environment during normal mammalian development (Dunwoodie, 2009) and is related to myogenesis in several vertebrates (Beaudry et al., 2016). Changes in environmental factors are clearly even more unpredictable for animals with external fertilization and development. For broadcast-spawning animals such as sea urchins, the gametes are released into the sea and embryogenesis takes place is a constantly changing environment. It remains unclear whether the intrinsic hypoxia gradient that we observed in the early embryo is relevant to the microenvironment that it is exposed to. Nevertheless, the differential levels of oxygen and mitochondrial activity might result in the gradients in metabolic rate that were thought by C. M. Child in the 1940s to be correlated with developmental potential and patterning

(Blackstone, 2006; Coffman and Denegre, 2007). Physiological hypoxia and the activation of the hypoxia pathway, leading to the stabilization of HIFα in sea urchins, represents an excellent example of linking environmental factors to transcriptional controls that are ultimately connected to a developmental GRN.

## MATERIALS AND METHODS

### Animals, embryos, cloning, and QPCR analysis

Adult sea urchins (*Strongylocentrotus purpuratus*) were obtained from Pat Leahy (Corona del Mar, CA, USA). Fertilization and embryo cultures were carried out in filtered seawater (FSW) at 15°C. Fragments of the sea urchin *hifα*, *hifβ*, *phda*, *phdb*, *fih* and *vhl* cDNAs were amplified by RT-PCR with primers designed based on sequence information in the genome database (Cameron et al., 2009), and the full-length sequences were then obtained by 5′ and 3′ RACE. The sequences have been deposited in GenBank with accession numbers KX786251-5 (*hifα*, *hifβ*, *phda*, *phdb* and *vhl*, respectively) and KX812732 (*fih*). The *hifα* sequence was translated, analyzed, and aligned using MacVector software (version 12.7.4). The coding sequence of *hifα* was subcloned into vectors pCS2+MT (Myc-tagged) and pCS2+8N-mCherry (Gokirmak et al., 2012). The mutated HIFα constructs were generated using the QuikChange site-directed mutagenesis kit with PfuTurbo DNA polymerase (Stratagene). The ODDD of HIFα was amplified and subcloned into the pBS-GFP vector (Oliveri et al., 2002). QPCR analyses were performed as previously described (Chen et al., 2011) using the primers listed in Table S1.

### Injections and treatments

mRNAs encoding Myc-HIFα, mutant forms of Myc-HIFα, Histone-GFP and HIFαODDD-GFP were *in vitro* transcribed using the mMESSAGE mMACHINE kit (Ambion) and injected into zygotes as previously described (Chang et al., 2016). For injection of the HRE-luciferase reporter (Addgene, 26731), the plasmid was linearized with *Bam*HI and mixed with *Hind*III-digested sea urchin genomic DNA. The efficacy of the translation-blocking HIFα MO (5′-GGTCGCCATAATCGGTCTCTGAATC-3′; GeneTools) has been tested using a *GFP* sequence fused with the MO target site. The Random Control 25-N (GeneTools), a mixture of many oligos, was injected as a control. For injections into one of the cells at the 2-cell stage, the fertilization envelopes were removed from zygotes by passing them through a 60 μm filter. The embryos were cultured until the first division occurred and then the culture medium was changed to $Ca^{2+}/Mg^{2+}$-free FSW before injections. MO or mRNA was mixed with 0.2 μg/μl Dextran-fluorescein (10,000 MW, D1820, ThermoFisher Scientific) and injected into one of the two cells. For the hypoxia treatment, FSW was equilibrated in a hypoxia chamber (ASTEC Water Jacket, APM-30DR) with 1% oxygen for 48 h before use. Zygotes were transferred into the equilibrated hypoxic FSW and incubated in the hypoxia chamber until collection for fixation. DMOG (Sigma-Aldrich) was dissolved in water and added to the embryo cultures (0.5 or 1 mM) after fertilization. To observe embryos clustered in rosettes, we arranged the embryos as previously described (Coffman and Davidson, 2001) before injection.

### Staining, imaging and image analyses

Immunostaining analyses were performed using antibodies against Myc (9E10, Santa Cruz, SC-40; 1:100), GFP (from Sheng-Ping L. Hwang, Institute of Cellular and Organismic Biology, Academia Sinica; 1:400), Vasa (Voronina et al., 2008) (1:50) and luciferase (Abcam, ab21176; 1:1000). The fixation and staining methods were as described previously (Luo and Su, 2012), except that the embryos that were used for Myc staining were fixed with 2% paraformaldehyde. To detect mitochondria, embryos were incubated with 0.1 μM MitoTracker Green FM (Invitrogen) for 30 min before observation. To monitor the intrinsic hypoxic signal, the fertilization envelope was removed and the embryos incubated with 400 μM pimonidazole for 2 h before fixation. Immunostaining was performed using antibodies against pimonidazole-protein adducts (Hypoxyprobe, Inc.; Hypoxyprobe-1 Omni Kit, rabbit 1:500; Hypoxyprobe-1 Kit, mouse 1:50). *In situ* hybridization analyses were performed following published

protocols. All images were generated on a Zeiss Axio Imager A1 or a Leica TCS-SP5 APBS confocal system. Images were analyzed using ImageJ (NIH) with plug-in programs. To quantify the fold differences between the strong and weak HIFα signals, we contoured the embryo and drew a line to separate the strong and weak regions. The fluorescence intensities (HIFα and GFP signals) were measured in both regions using 'region measure' of MetaMorph software (Molecular Devices). The fold differences were then calculated by: (HIFα intensity on the strong side/GFP intensity on the strong side)/(HIFα intensity on the weak side/GFP intensity on the weak side).

### Author contributions

Conceptualization: W.-L.C., Y.-C.C., Y.-H.S.; Methodology: W.-L.C., Y.-C.C., K.-T.L., Y.-H.S.; Software: W.-L.C., Y.-C.C.; Validation: W.-L.C., Y.-C.C., H.-R.L., C.-Y.P.; Formal analysis: W.-L.C., Y.-C.C., K.-T.L., H.-R.L., C.-Y.P., J.-H.C., Y.-H.S.; Investigation: W.-L.C., Y.-C.C., K.-T.L., H.-R.L., C.-Y.P., J.-H.C., Y.-H.S.; Resources: Y.-H.S.; Data curation: W.-L.C., Y.-C.C., Y.-H.S.; Writing - original draft: Y.-H.S.; Writing - review & editing: Y.-H.S.; Visualization: Y.-H.S.; Supervision: Y.-H.S.; Project administration: Y.-H.S.; Funding acquisition: Y.-H.S.

### Data availability

*Strongylocentrotus purpuratus* gene sequences have been deposited in GenBank under the following accession numbers: *hifα*, KX786251; *hifβ*, KX786252; *phda*, KX786253; *phdb*, KX786254; *vhl*, KX786255; and *fih*, KX812732.

### Supplementary information

Supplementary information available online at
http://dev.biologists.org/lookup/doi/10.1242/dev.145052.supplemental

### References

**Agca, C., Klein, W. H. and Venuti, J. M.** (2009). Reduced O₂ and elevated ROS in sea urchin embryos leads to defects in ectoderm differentiation. *Dev. Dyn.* **238**, 1777-1787.

**Beaudry, M., Hidalgo, M., Launay, T., Bello, V. and Darribère, T.** (2016). Regulation of myogenesis by environmental hypoxia. *J. Cell Sci.* **129**, 2887-2896.

**Beldade, P., Mateus, A. R. A. and Keller, R. A.** (2011). Evolution and molecular mechanisms of adaptive developmental plasticity. *Mol. Ecol.* **20**, 1347-1363.

**Bell, E. L., Klimova, T. A., Eisenbart, J., Moraes, C. T., Murphy, M. P., Budinger, G. R. S. and Chandel, N. S.** (2007). The Qo site of the mitochondrial complex III is required for the transduction of hypoxic signaling via reactive oxygen species production. *J. Cell Biol.* **177**, 1029-1036.

**Ben-Tabou de-Leon, S., Su, Y.-H., Lin, K.-T., Li, E. and Davidson, E. H.** (2013). Gene regulatory control in the sea urchin aboral ectoderm: spatial initiation, signaling inputs, and cell fate lockdown. *Dev. Biol.* **374**, 245-254.

**Blackstone, N. W.** (2006). Charles Manning Child (1869-1954): the past, present, and future of metabolic signaling. *J. Exp. Zool. B Mol. Dev. Evol.* **306B**, 1-7.

**Bradham, C. A. and Mcclay, D. R.** (2006). p38 MAPK is essential for secondary axis specification and patterning in sea urchin embryos. *Development* **133**, 21-32.

**Cameron, R. A., Fraser, S. E., Britten, R. J. and Davidson, E. H.** (1989). The oral-aboral axis of a sea urchin embryo is specified by first cleavage. *Development* **106**, 641-647.

**Cameron, R. A., Samanta, M., Yuan, A., He, D. and Davidson, E.** (2009). SpBase: the sea urchin genome database and web site. *Nucleic Acids Res.* **37**, D750-D754.

**Carreau, A., El Hafny-Rahbi, B., Matejuk, A., Grillon, C. and Kieda, C.** (2011). Why is the partial oxygen pressure of human tissues a crucial parameter? Small molecules and hypoxia. *J. Cell. Mol. Med.* **15**, 1239-1253.

**Centanin, L., Ratcliffe, P. J. and Wappner, P.** (2005). Reversion of lethality and growth defects in Fatiga oxygen-sensor mutant flies by loss of hypoxia-inducible factor-alpha/Sima. *EMBO Rep.* **6**, 1070-1075.

**Chang, Y.-C., Pai, C.-Y., Chen, Y.-C., Ting, H.-C., Martinez, P., Telford, M. J., Yu, J.-K. and Su, Y.-H.** (2016). Regulatory circuit rewiring and functional divergence of the duplicate admp genes in dorsoventral axial patterning. *Dev. Biol.* **410**, 108-118.

Chen, H. and Shi, H. (2008). A reducing environment stabilizes HIF-2alpha in SH-SY5Y cells under hypoxic conditions. *FEBS Lett.* **582**, 3899-3902.

Chen, J.-H., Luo, Y.-J. and Su, Y.-H. (2011). The dynamic gene expression patterns of transcription factors constituting the sea urchin aboral ectoderm gene regulatory network. *Dev. Dyn.* **240**, 250-260.

Child, C. M. (1941). Formation and reduction of indophenol blue in development of an echinoderm. *Proc. Natl. Acad. Sci. USA* **27**, 523-528.

Coffman, J. A. and Davidson, E. H. (2001). Oral-aboral axis specification in the sea urchin embryo. I. Axis entrainment by respiratory asymmetry. *Dev. Biol.* **230**, 18-28.

Coffman, J. A. and Denegre, J. M. (2007). Mitochondria, redox signaling and axis specification in metazoan embryos. *Dev. Biol.* **308**, 266-280.

Coffman, J. A., Mccarthy, J. J., Dickey-Sims, C. and Robertson, A. J. (2004). Oral-aboral axis specification in the sea urchin embryo II. Mitochondrial distribution and redox state contribute to establishing polarity in Strongylocentrotus purpuratus. *Dev. Biol.* **273**, 160-171.

Coffman, J. A., Wessels, A., Deschiffart, C. and Rydlizky, K. (2014). Oral-aboral axis specification in the sea urchin embryo, IV: hypoxia radializes embryos by preventing the initial spatialization of nodal activity. *Dev. Biol.* **386**, 302-307.

Coluccio, A. E., Lacasse, T. J. and Coffman, J. A. (2011). Oxygen, pH, and oral-aboral axis specification in the sea urchin embryo. *Mol. Reprod. Dev.* **78**, 68.

Compernolle, V., Brusselmans, K., Acker, T., Hoet, P., Tjwa, M., Beck, H., Plaisance, S., Dor, Y., Keshet, E., Lupu, F. et al. (2002). Loss of HIF-2alpha and inhibition of VEGF impair fetal lung maturation, whereas treatment with VEGF prevents fatal respiratory distress in premature mice. *Nat. Med.* **8**, 702-710.

Czihak, G. (1963). Entwicklungsphysiologische Untersuchungen an Echiniden (Verteilung und Bedeutung der Cytochromoxydase). *Roux' Arch. Entwickl. Mech. Dev.* **154**, 272-292.

Davidson, E. H. (2006). *The Regulatory Genome: Gene Regulatory Networks in Development and Evolution.* San Diego: Academic Press.

De Smedt, V., Szöllösi, D. and Kloc, M. (2000). The balbiani body: asymmetry in the mammalian oocyte. *Genesis* **26**, 208-212.

Duan, C. (2016). Hypoxia-inducible factor 3 biology: complexities and emerging themes. *Am. J. Physiol. Cell Physiol.* **310**, C260-C269.

Dunwoodie, S. L. (2009). The role of hypoxia in development of the mammalian embryo. *Dev. Cell* **17**, 755-773.

Foxler, D. E., Bridge, K. S., James, V., Webb, T. M., Mee, M., Wong, S. C. K., Feng, Y., Constantin-Teodosiu, D., Petursdottir, T. E., Bjornsson, J. et al. (2012). The LIMD1 protein bridges an association between the prolyl hydroxylases and VHL to repress HIF-1 activity. *Nat. Cell Biol.* **14**, 201-208.

Gildor, T. and Ben-Tabou de-Leon, S. (2015). Comparative study of regulatory circuits in two sea urchin species reveals tight control of timing and high conservation of expression dynamics. *PLoS Genet.* **11**, e1005435.

Gökirmak, T., Campanale, J. P., Shipp, L. E., Moy, G. W., Tao, H. and Hamdoun, A. (2012). Localization and substrate selectivity of sea urchin multidrug (MDR) efflux transporters. *J. Biol. Chem.* **287**, 43876-43883.

Gomes, A. P., Price, N. L., Ling, A. J. A., Moslehi, J. J., Montgomery, M. K., Rajman, L., White, J. P., Teodoro, J. S., Wrann, C. D., Hubbard, B. P. et al. (2013). Declining NAD(+) induces a pseudohypoxic state disrupting nuclear-mitochondrial communication during aging. *Cell* **155**, 1624-1638.

Gray, J. M., Karow, D. S., Lu, H., Chang, A. J., Chang, J. S., Ellis, R. E., Marletta, M. A. and Bargmann, C. I. (2004). Oxygen sensation and social feeding mediated by a C. elegans guanylate cyclase homologue. *Nature* **430**, 317-322.

Guo, S., Bragina, O., Xu, Y., Cao, Z., Chen, H., Zhou, B., Morgan, M., Lin, Y., Jiang, B.-H., Liu, K. J. et al. (2008). Glucose up-regulates HIF-1 alpha expression in primary cortical neurons in response to hypoxia through maintaining cellular redox status. *J. Neurochem.* **105**, 1849-1860.

Haillot, E., Molina, M. D., Lapraz, F. and Lepage, T. (2015). The maternal maverick/GDF15-like TGF-beta ligand panda directs dorsal-ventral axis formation by restricting nodal expression in the sea urchin embryo. *PLoS Biol.* **13**, e1002247.

Iyer, N. V., Kotch, L. E., Agani, F., Leung, S. W., Laughner, E., Wenger, R. H., Gassmann, M., Gearhart, J. D., Lawler, A. M., Yu, A. Y. et al. (1998). Cellular and developmental control of O2 homeostasis by hypoxia-inducible factor 1 alpha. *Genes Dev.* **12**, 149-162.

Jiang, H., Guo, R. and Powell-Coffman, J. A. (2001). The Caenorhabditis elegans hif-1 gene encodes a bHLH-PAS protein that is required for adaptation to hypoxia. *Proc. Natl. Acad. Sci. USA* **98**, 7916-7921.

Kaelin, W. G., Jr. and Ratcliffe, P. J. (2008). Oxygen sensing by metazoans: the central role of the HIF hydroxylase pathway. *Mol. Cell* **30**, 393-402.

Kloc, M., Bilinski, S., Chan, A. P., Allen, L. H., Zearfoss, N. R. and Etkin, L. D. (2001). RNA localization and germ cell determination in Xenopus. *Int. Rev. Cytol.* **203**, 63-91.

Kloc, M., Jedrzejowska, I., Tworzydlo, W. and Bilinski, S. M. (2014). Balbiani body, nuage and sponge bodies–term plasm pathway players. *Arthropod Struct. Dev.* **43**, 341-348.

Lapraz, F., Haillot, E. and Lepage, T. (2015). A deuterostome origin of the Spemann organiser suggested by Nodal and ADMPs functions in echinoderms. *Nat. Commun.* **6**, 8434.

Loenarz, C., Coleman, M. L., Boleininger, A., Schierwater, B., Holland, P. W. H., Ratcliffe, P. J. and Schofield, C. J. (2011). The hypoxia-inducible transcription factor pathway regulates oxygen sensing in the simplest animal, Trichoplax adhaerens. *EMBO Rep.* **12**, 63-70.

Luo, Y.-J. and Su, Y.-H. (2012). Opposing Nodal and BMP signals regulate left-right asymmetry in the sea urchin larva. *PLoS Biol.* **10**, e1001402.

Nam, J., Su, Y.-H., Lee, P. Y., Robertson, A. J., Coffman, J. A. and Davidson, E. H. (2007). Cis-regulatory control of the nodal gene, initiator of the sea urchin oral ectoderm gene network. *Dev. Biol.* **306**, 860-869.

Oliveri, P., Carrick, D. M. and Davidson, E. H. (2002). A regulatory gene network that directs micromere specification in the sea urchin embryo. *Dev. Biol.* **246**, 209-228.

Pease, D. C. (1941). Echinoderm bilateral determination in chemical concentration gradients I The effects of cyanide, ferricyanide, iodoacetate, picrate, dinitrophenol, urethane, iodine, malonate, etc. *J. Exp. Zool.* **86**, 381-404.

Pease, D. C. (1942a). Echinoderm bilateral determination in chemical concentration gradients II The effects of azide, pilocarpine, pyocyanine, diamine, cysteine, glutathione, and lithium. *J. Exp. Zool.* **89**, 329-345.

Pease, D. C. (1942b). Echinoderm bilateral determination in chemical concentration gradients III The effects of carbon monoxide and other gases. *J. Exp. Zool.* **89**, 347-356.

Peng, J., Zhang, L., Drysdale, L. and Fong, G.-H. (2000). The transcription factor EPAS-1/hypoxia-inducible factor 2alpha plays an important role in vascular remodeling. *Proc. Natl. Acad. Sci. USA* **97**, 8386-8391.

Poyton, R. O., Ball, K. A. and Castello, P. R. (2009). Mitochondrial generation of free radicals and hypoxic signaling. *Trends Endocrinol. Metab.* **20**, 332-340.

Range, R., Lapraz, F., Quirin, M., Marro, S., Besnardeau, L. and Lepage, T. (2007). Cis-regulatory analysis of nodal and maternal control of dorsal-ventral axis formation by Univin, a TGF-beta related to Vg1. *Development* **134**, 3649-3664.

Rankin, E. B. and Giaccia, A. J. (2016). Hypoxic control of metastasis. *Science* **352**, 175-180.

Ryan, H. E., Lo, J. and Johnson, R. S. (1998). HIF-1 alpha is required for solid tumor formation and embryonic vascularization. *EMBO J.* **17**, 3005-3015.

Rytkönen, K. T., Williams, T. A., Renshaw, G. M., Primmer, C. R. and Nikinmaa, M. (2011). Molecular evolution of the metazoan PHD-HIF oxygen-sensing system. *Mol. Biol. Evol.* **28**, 1913-1926.

Safran, M., Kim, W. Y., O'connell, F., Flippin, L., Gunzler, V., Horner, J. W., Depinho, R. A. and Kaelin, W. G.Jr. (2006). Mouse model for noninvasive imaging of HIF prolyl hydroxylase activity: assessment of an oral agent that stimulates erythropoietin production. *Proc. Natl. Acad. Sci. USA* **103**, 105-110.

Sardet, C., Paix, A., Prodon, F., Dru, P. and Chenevert, J. (2007). From oocyte to 16-cell stage: cytoplasmic and cortical reorganizations that pattern the ascidian embryo. *Dev. Dyn.* **236**, 1716-1731.

Saudemont, A., Haillot, E., Mekpoh, F., Bessodes, N., Quirin, M., Lapraz, F., Duboc, V., Röttinger, E., Range, R., Oisel, A. et al. (2010). Ancestral regulatory circuits governing ectoderm patterning downstream of Nodal and BMP2/4 revealed by gene regulatory network analysis in an echinoderm. *PLoS Genet.* **6**, e1001259.

Schofield, C. J. and Ratcliffe, P. J. (2004). Oxygen sensing by HIF hydroxylases. *Nat. Rev. Mol. Cell Biol.* **5**, 343-354.

Scortegagna, M., Ding, K., Oktay, Y., Gaur, A., Thurmond, F., Yan, L.-J., Marck, B. T., Matsumoto, A. M., Shelton, J. M., Richardson, J. A. et al. (2003). Multiple organ pathology, metabolic abnormalities and impaired homeostasis of reactive oxygen species in Epas1-/- mice. *Nat. Genet.* **35**, 331-340.

Semenza, G. L. (2000). HIF-1 and human disease: one highly involved factor. *Genes Dev.* **14**, 1983-1991.

Semenza, G. L. (2007). Life with oxygen. *Science* **318**, 62-64.

Shih, S.-C. and Claffey, K. P. (2001). Role of AP-1 and HIF-1 transcription factors in TGF-beta activation of VEGF expression. *Growth Factors* **19**, 19-34.

Simon, M. C. and Keith, B. (2008). The role of oxygen availability in embryonic development and stem cell function. *Nat. Rev. Mol. Cell Biol.* **9**, 285-296.

Su, Y.-H., Li, E., Geiss, G. K., Longabaugh, W. J. R., Krämer, A. and Davidson, E. H. (2009). A perturbation model of the gene regulatory network for oral and aboral ectoderm specification in the sea urchin embryo. *Dev. Biol.* **329**, 410-421.

Tian, H., Hammer, R. E., Matsumoto, A. M., Russell, D. W. and Mcknight, S. L. (1998). The hypoxia-responsive transcription factor EPAS1 is essential for catecholamine homeostasis and protection against heart failure during embryonic development. *Genes Dev.* **12**, 3320-3324.

Varia, M. A., Calkins-Adams, D. P., Rinker, L. H., Kennedy, A. S., Novotny, D. B., Fowler, W. C., Jr. and Raleigh, J. A. (1998). Pimonidazole: a novel hypoxia marker for complementary study of tumor hypoxia and cell proliferation in cervical carcinoma. *Gynecol. Oncol.* **71**, 270-277.

Voronina, E., Lopez, M., Juliano, C. E., Gustafson, E., Song, J. L., Extavour, C., George, S., Oliveri, P., Mcclay, D. and Wessel, G. (2008). Vasa protein expression is restricted to the small micromeres of the sea urchin, but is inducible in other lineages early in development. *Dev. Biol.* **314**, 276-286.

Wenger, R. H., Stiehl, D. P. and Camenisch, G. (2005). Integration of oxygen signaling at the consensus HRE. *Sci. STKE* **2005**, re12.

DEVELOPMENT